NASA TECHNICAL NOTE

NASA TN D-2676

NASA TN D-2676

EXPERIMENTAL INVESTIGATION OF A CONSTANT-VELOCITY TRAVELING MAGNETIC WAVE PLASMA ENGINE

by Robert E. Jones and Raymond W. Palmer

Lewis Research Center
Cleveland, Ohio

NATIONAL AERONAUTICS AND SPACE ADMINISTRATION • WASHINGTON, D. C. • FEBRUARY 1965

EXPERIMENTAL INVESTIGATION OF A CONSTANT-VELOCITY TRAVELING MAGNETIC WAVE PLASMA ENGINE

By Robert E. Jones and Raymond W. Palmer

Lewis Research Center
Cleveland, Ohio

NATIONAL AERONAUTICS AND SPACE ADMINISTRATION

For sale by the Office of Technical Services, Department of Commerce,
Washington, D.C. 20230 -- Price $1.00

EXPERIMENTAL INVESTIGATION OF A CONSTANT-VELOCITY TRAVELING MAGNETIC WAVE PLASMA ENGINE*

by Robert E. Jones and Raymond W. Palmer

Lewis Research Center

SUMMARY

The previously reported traveling magnetic wave plasma engine has been redesigned to reduce the high heat loss to the tube walls downstream of the last magnetic-field coil. The present configuration uses a 3-inch-diameter pyrex tube flared out to a 6-inch diameter immediately downstream of the last magnetic-field coil. This configuration has been studied to determine the effects of flared-tube geometry, molecular weight of the propellant, engine length, and use of a ferrite core on the engine performance. Argon and xenon gases were used as propellants. Two engine lengths were tested. One engine was nominally 1-magnetic-wavelength long (4 coils) and the other nominally $2\frac{1}{2}$-magnetic-wavelengths long (10 coils). The magnetic wave speed for both of these lengths corresponds to a specific impulse of 4750 seconds. The maximum kinetic efficiency of the 4-coil engine was 10 percent at a specific impulse of 3200 seconds using argon gas and 22.5 percent at 4200 seconds using xenon gas as the propellant.

Increasing the engine length had a negligible effect on the performance with argon gas; however, the increased engine length resulted in lowered performance with xenon gas. It appears that there may be an optimum engine length that will yield maximum efficiency for each propellant.

The efficiency of the 4-coil engine with the ferrite core installed was significantly lower than that obtained when no core was used. Drag and heat losses caused by the core exceeded any positive effect produced by enhancing the radial component of the magnetic field.

---

*An abbreviated version of this report was presented at the Fifth Symposium on The Engineering Aspects of Magnetohydrodynamics, Massachusetts Institute of Technology, April 1-2, 1964.

INTRODUCTION

The traveling magnetic wave plasma engine is one of several devices being investigated for possible use as a thrustor for electric propulsion systems. This concept is analagous to alternating-current induction motors, the principle difference being the use of a gaseous, rather than a solid, conductor as the moving element. Operation is based on the production of a moving magnetic wave, which passes through the plasma and induces a current within it. The interaction of the induced current and the applied magnetic field produces a body force that tends to accelerate the plasma in the direction of the moving magnetic wave.

A more detailed consideration of the nature of the accelerating force shows that, of the three constituents of the plasma (electrons, ions, and neutrals), only the electrons are mobile enough to be affected by magnetic waves of the strengths normally employed. This preferential acceleration of electrons creates an electrostatic potential that accelerates the ions. The ions, in turn, impart forward momentum to neutral particles through collisions. Thus, the entire propellant stream can be accelerated to a certain fraction of the magnetic-wave velocity.

A variety of configurations has been used for experimental research on this concept. These configurations differ essentially only in the technique for the production of the moving magnetic wave. Schaffer (ref. 1) describes a "lumped-parameter" transmission line for pulsed operation. A similar transmission line approach has been studied by Covert and Haldemann (ref. 2) for continuous power application. A coaxial-coil geometry excited with polyphase current was used by the present authors to generate the constant-velocity magnetic wave plasma engine described in reference 3. A coaxial, polyphased coil system mounted on an expanding conical tube was used by Smotrich and Janes (ref. 4) to produce a slowly accelerating wave. An interesting attempt to create a high-strength transverse magnetic field was tried by Heflinger and Schaffer (refs. 5 and 6) by arranging coils in pairs perpendicular to the plasma stream. Though each of these wave-producing systems has its particular merits, it is not yet clear which system is the most efficient.

Presented herein are the experimental results of several modifications employed to improve the performance of the plasma engine of reference 3. That engine consisted of four magnetic-field coils mounted on a constant-diameter pyrex tube, which produced a constant-velocity magnetic wave. This engine configuration exhibited very low efficiency (1 percent) primarily due to the very high heat losses to the tube walls, which, for the most part, occurred just downstream of the last field coil. The first modification introduced was a redesign of the plasma tube to incorporate a flared section immediately downstream of the last field coil. This design change also reduced the tendency of the pyrex tube to break as a result of thermal stresses and so was used throughout this

entire investigation. Another approach for reducing the heat-transfer losses was to use a higher molecular weight propellant, xenon rather than argon, thereby decreasing the diffusion rate of the plasma to the tube walls.

The effect of engine length was also studied by increasing the number of wavelengths available for plasma acceleration from 1 to $2\frac{1}{2}$. For constant spacing between coils, this wavelength increase required a corresponding increase in the number of coils from 4 to 10. The effect of propellant molecular weight was tested with this longer engine by using both argon and xenon gases alternately as the propellants.

A ferrite core was installed on the axis of the 4-coil engine in a further attempt to increase the engine efficiency. This core increased the strength of the radial component of the magnetic wave. For comparison purposes, a similar core, but with no ferrite in it, was tested. Both of these tests were made with only xenon gas as the propellant.

APPARATUS

Engine Installation

The traveling magnetic wave plasma engine was externally mounted on one of the large vacuum tanks described in detail in reference 7. This particular 5-foot-diameter 16-foot-long tank was equipped with four 32-inch-diameter oil diffusion pumps capable of maintaining a pressure of 0.8×10^{-5} to 4.5×10^{-5} torr at the plasma flow rates used in these tests. A minimum tank pressure of 8×10^{-8} torr was obtainable with no gas flow. The plasma engine was connected to the vacuum tank through a 12-inch-diameter gate valve.

Engine Configurations

Four-coil engine. - The 4-coil four-phase traveling magnetic wave plasma engine was designed on the basis of the results of the magnetic wave analysis of reference 8 and is shown schematically in figure 1(a). The four magnetic-field coils were equally spaced along a 3-inch-diameter pyrex tube. A 3- to 6-inch pyrex flared section was fused to one end of the 3-inch-diameter tube and connected to a 6-inch-diameter pyrex tee. The pyrex tee was used as an instrumentation section and connected the plasma engine to the gate valve on the vacuum tank. Both the pyrex tube and the flared section were enclosed within a plastic jacket for water-cooling the tube walls.

The magnetic-field coils were spaced 3.06 inches apart, center to center, with the last coil positioned as close as possible to the end of the 3-inch-diameter tube. This

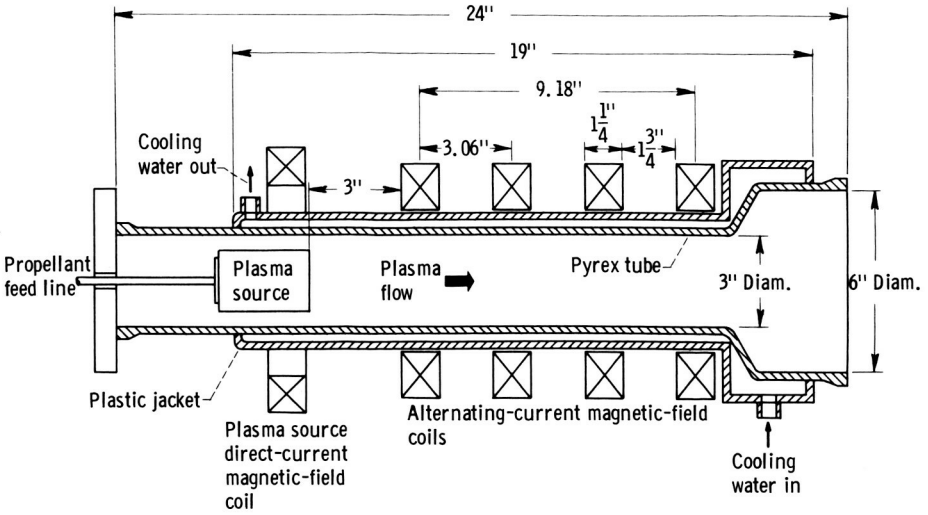

(a) Cutaway drawing.

(b) Engine in operation.

Figure 1. - Four-coil four-phase traveling magnetic wave plasma engine.

minimized the length of tubing that extended beyond the last coil and therefore minimized the heat lost to the tube walls at that point. The spacing for the magnetic-field coils was calculated from the optimum value of the coil-radius to magnetic-wave-wavelength ratio, as determined from reference 8. This coil spacing and the operating frequency of 150 kilocycles fix the velocity of the magnetic wave at 4.65×10^4 meters per second.

The 4-coil four-phase traveling magnetic wave plasma engine in operation is shown in figure 1(b).

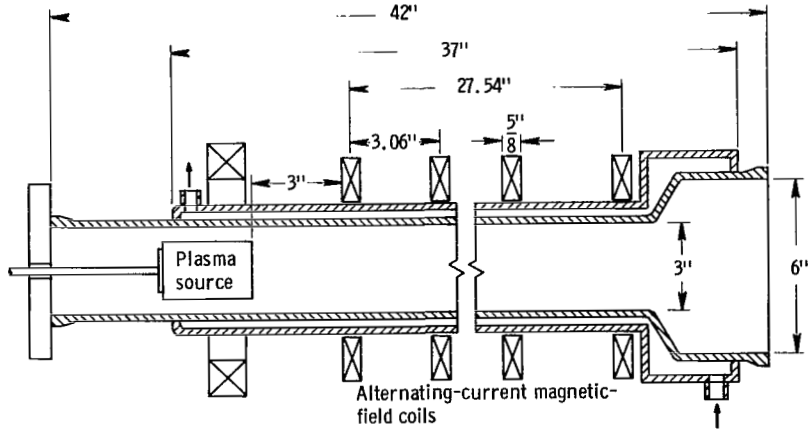

Figure 2. - Cutaway drawing of 10-coil four-phase traveling magnetic wave plasma engine.

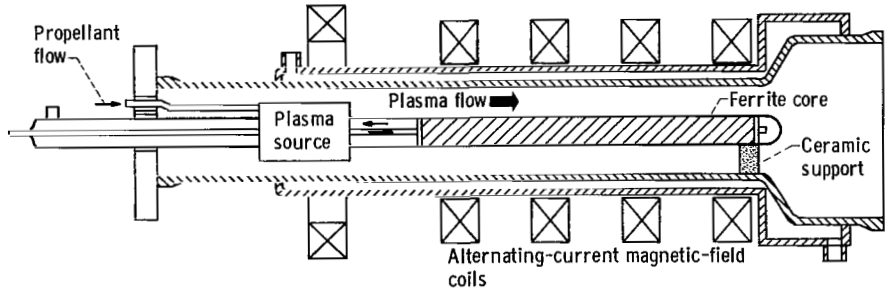

(a) Cutaway drawing showing location of ferrite core.

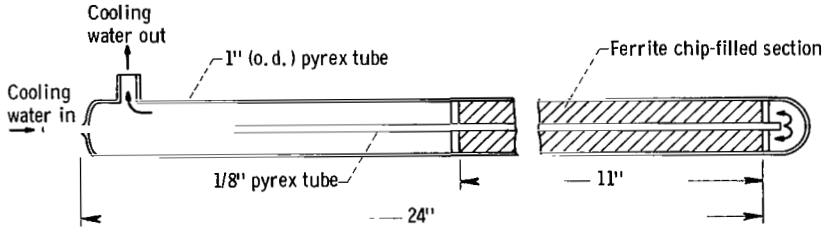

(b) Cutaway drawing of ferrite core.

Figure 3. - Four-coil four-phase ferrite core traveling magnetic wave plasma engine.

Ten-coil engine. - Figure 2 is a cutaway drawing of the 10-coil engine. The coils were equally spaced along the pyrex tube in the same manner as in the 4-coil engine. Thus, $2\frac{1}{2}$ wavelengths were available for plasma acceleration. Since the coil spacings and operating frequency were identical to those used in the 4-coil engine the velocity was the same, 4.65×10^4 meters per second.

Ferrite-core engine. - A ferrite core was installed on the centerline of the 4-coil engine in an attempt to increase the engine performance by increasing the strength of the radial component of the magnetic wave. Figure 3(a) is a cutaway drawing of the engine showing the location of the core, and figure 3(b) shows details of the core construction.

A ferritic material was chosen in preference to a laminated iron core to avoid any power losses in the core due to eddy current heating. The core was made by packing ferrite chips into a 1-inch-diameter closed-end pyrex tube for a distance of 11 inches. The ferrite portion of the core was centered under the 4 coils and supported at the downstream end with a small ceramic block. Constant thermal properties of the ferrite core were assured by circulating cooling water through the core. For comparison purposes, data were also taken with an identical, empty, air-cooled pyrex core in place of the ferrite core.

Engine Components

Magnetic-field coils. - The magnetic-field coils used for the 4-coil and 10-coil engines were wound with 1/4-inch-diameter polyethylene-coated copper tubing. The inside diameter of these coils was $4\frac{3}{8}$ inches, and the outside diameter was $7\frac{1}{2}$ inches. The coils for the 4-coil engine had 20 turns, wound 4 turns long by 5 turns high, while those for the 10-coil engine had 10 turns, wound 2 turns long by 5 turns high. The inductance of the 20-turn and 10-turn coils was approximately 65 and 16.5 microhenries, respectively. During operation, these coils were cooled with distilled water. The water flow rate and the inlet and outlet water temperatures were recorded to measure the power consumed in the magnetic-field coils.

Plasma source. - The direct-current plasma source was installed in the pyrex tube 3 inches upstream of the first magnetic-field coil, as shown in figures 1 to 3. A schematic diagram of the plasma source is shown in figure 4, and a more complete discussion of the construction and operation of the source is given by Domitz (ref. 9). Briefly, this plasma source operates as follows: Electrons, emitted from the filament, are forced into spiral paths to the anode by an imposed steady magnetic field. The propellant is admitted through a baffle at the rear of the source and becomes ionized by collisions with the electrons. The resultant partially ionized plasma diffuses out of the source and into the region of the traveling magnetic wave.

Power supply. - The radio-frequency power for the magnetic-field coils was supplied by two 13-kilowatt transmitters operating at a frequency of 150 kilocycles per second. Figure 5 shows the electrical connection of the output stage of one of the transmitters to the impedance matching network and the magnetic-field coils. The current output of the two transmitters was maintained 90° apart in electrical phase angle by adjusting the variable capacitors in each of the matching networks. Enough capacitance was provided in each circuit to adjust for changes in the circuit impedance due to the plasma loading.

Each radio-frequency transmitter supplied power to half of the engine coils plus one

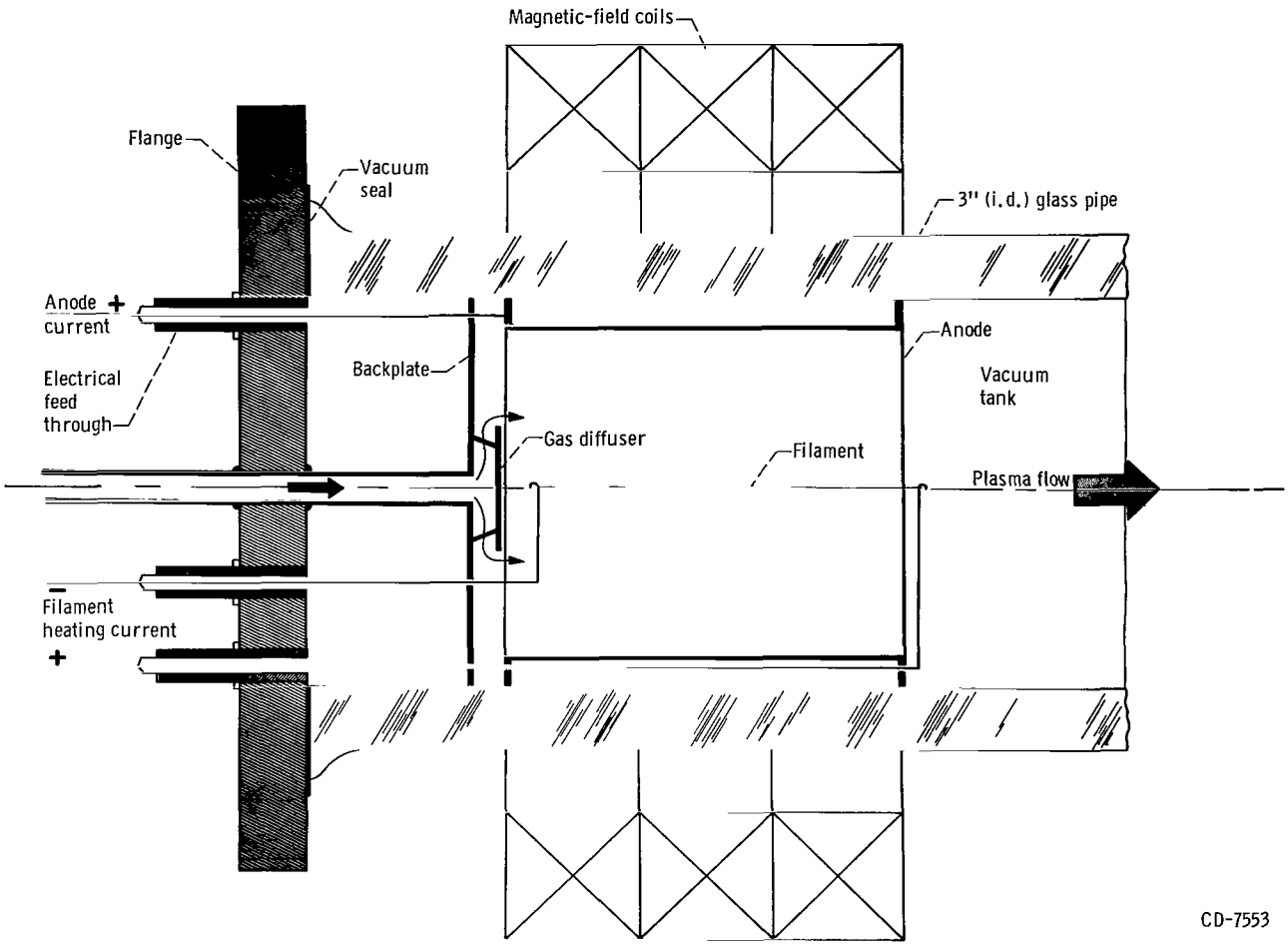

Figure 4. - Schematic diagram of traveling magnetic wave plasma source.

externally located coil. The two externally located coils were so arranged that the spacing between them could be varied in order to cancel the mutual interaction between the coils mounted on the tube. The direction of the windings of the four magnetic-field coils was so adjusted that the electrical current phase angle increased linearly along the engine. The linear variation of the phase means that the magnetic wave travels at a constant velocity.

Instrumentation

Radio-frequency meters. - The power metering shown in the electrical diagram of figure 5 consisted of a directional coupler that supplied signals to two alternating-current millivoltmeters. These meters were calibrated to read forward and reverse radio-frequency powers. Coil currents were read from calibrated alternating-current volt-

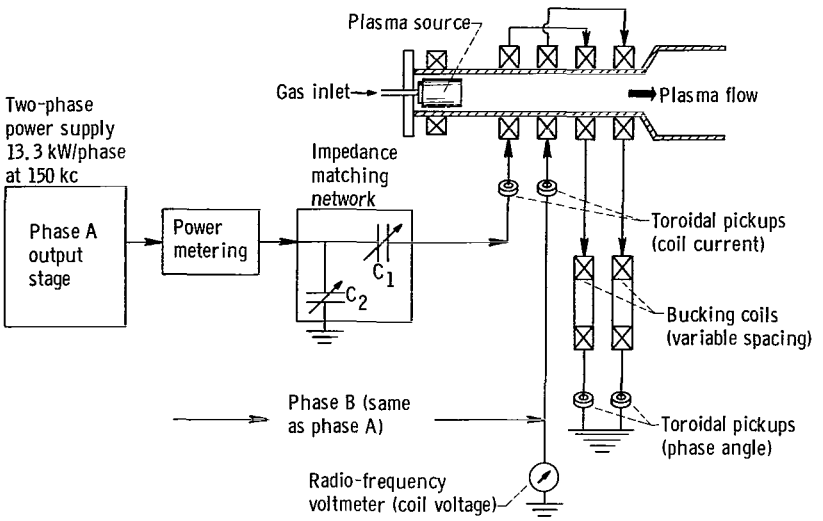

Figure 5. - Electrical instrumentation and matching network for traveling magnetic wave plasma engine.

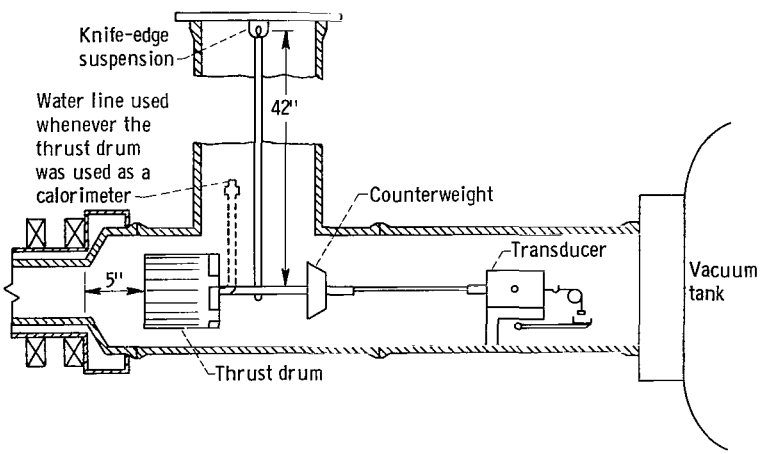

Figure 6. - Thrust measurement instrumentation and its location relative to traveling magnetic wave plasma engine.

meters. The signals to these voltmeters were supplied by ferrite-core toroids. The electrical phase angle between the two phases was measured with a standard high-frequency phase-angle meter. The reference signals for the phase meter were obtained from toroidal pickups, as shown in figure 5. The high-frequency voltage of the phase B resonant circuit was monitored with a radio-frequency voltmeter.

Propellant flow. - The propellant gases used were commercially available argon and xenon. The gas flow rate was measured with a calibrated rotameter and was admitted to the engine through the plasma source.

Thrust measurement. - Figure 6 shows the thrust measurement instrumentation indicating its location relative to the engine. The thrust drum was mounted so that there was a 5-inch clearance between the exit of the plasma engine and the leading edge of the

drum. The drum and its counterweight were fastened to a 3/8-inch-diameter steel tube, 42 inches long, which was suspended to act as a pendulum. A thin ceramic rod connected the target pendulum to a linear, variable, differential transformer, which was calibrated to read thrust directly. The calibration was accomplished by suspending small weights over a pulley to the transducer. A vacuum actuator was fitted through one flange of the 6-inch cross so that the calibration could be checked in vacuum by lowering a 2-gram weight over the pulley. The thrust target sensitivity was usually adjusted to be 1.96×10^{-2} newton, full scale. The minimum detectable thrust was approximately 4×10^{-4} newton or 2 percent of full scale. More accurate readings could not usually be obtained due to the high background vibration level.

The thrust drum was constructed of a 1/32-inch-thick copper sheet rolled into a 4-inch-diameter cylinder, 4 inches long and sealed with a thin copper disk at one end. The drum was slotted at approximately 1-inch intervals on the circumference to prevent large circulating currents from being induced in the drum. There were five ports, perpendicular to the direction of the entering flow, cut into the side of the drum at the sealed base to duct the plasma out of the drum. The total open area of these ports was slightly greater than the capture area of the thrust drum.

Beam power. - Plasma-beam-power measurements were made by using the thrust drum as a calorimeter. The inside of the drum and the back plate were wrapped with 1/8-inch-diameter copper tubing. A metered, continuous flow of water cooled the drum. Thermocouple measurement of the temperature difference between the inlet and outlet water streams was amplified and displayed on a strip-chart recorder. The calorimeter was sensitive to temperature changes as low as 0.25° F and responded with a time constant of approximately 12 seconds.

In operation, the thrust drum was not used to measure thrust and beam power simultaneously, because the cooling water introduced a heat-dependent force reading that made accurate thrust determination impossible.

Streak photographs. - High-speed streak photographs, taken with a commercially available image-converter camera that could be used in either a streak or a framing mode, of the 4-coil engine were made in an attempt to determine the velocity of the plasma stream. Typical streak-camera exposure times were of 5- or 10-microseconds duration. Xenon gas was used as the propellant during these photographic studies to obtain a discharge of sufficient light intensity to yield usable pictures. The engine was completely covered with an opaque cloth except for a 1-inch-wide slot at the centerline running the entire length of the engine. This slot in the covering material served as the viewing slit for the streak photographs.

Streak photographs were taken either of the entire engine or of the region between the second and third magnetic-field coils. The region between these two coils was selected for study because the magnetic wave is most uniform through this portion of the

engine. Although the discharge is quite bright with xenon, there was not sufficient luminosity in the exhaust stream (i. e., downstream of the last driver coil) to obtain usable pictures.

PROCEDURE

Operating Conditions

The traveling magnetic wave plasma engine performance was evaluated over the following range of operating conditions:

Propellant mass flow rate, kg/sec	
Argon	0.26×10^{-6} to 1.98×10^{-6}
Xenon	0.21×10^{-6} to 2.64×10^{-6}
Magnetic-field coil current, rms A	
4-Coil engine	35 to 45
10-Coil engine	40 to 70
Magnetic wave speed, m/sec	46 500
Operating frequency, cps	150 000
Maximum available power, W	26 600
Pressure in 6-inch tee (engine exhaust pressure), torr	0.1×10^{-3} to 4×10^{-3}

The axial magnetic-field strength on the centerline of the 4-coil engine was 76.5 rms gauss at a field coil current of 45 rms amperes. The engine was not operated with simultaneously high propellant flow rates and currents due to the very rapid heating of the pyrex tube.

Test Procedure

The test procedure during a typical data-gathering run was as follows: After the propellant mass flow rate was set to the desired value on the gas rotameter, the thrust target was zeroed and the calibration was checked. Then the plasma source was turned on, and the anode current was adjusted to 1 ampere by varying the heater current to the filament. For some runs, particularly those using xenon gas, the plasma source was not required to start the discharge, and its use was often omitted. The use or omission of the plasma source during operation in no way affected the engine performance. The two transmitters were turned on, and the plasma engine coil currents raised to a predetermined value. Adjustment of the variable capacitors in the matching network of

each electrical phase was then made to minimize the reflected power and correct the current phase angle to 90°. When this condition was reached, data were taken. As soon as all the pertinent data had been recorded, the radio-frequency current was lowered to zero. Generally, the total time required for such a test run was about 2 minutes. This time was too short for the entire system to come to thermal equilibrium; thus, heat-loss determinations using the cooling-jacket water temperature rise were not usually attempted. This operating procedure was not significantly altered when the thrust drum was used as a calorimeter.

Calculations

A thrust efficiency was calculated on the basis of measured thrust, propellant mass flow rate, and power transmitted to the gas. This thrust efficiency, or kinetic efficiency, is given by

$$\eta_T = \frac{T^2}{2\dot{m}P_G} \tag{1}$$

where

T	thrust, N
$\dot{m}$	propellant mass flow rate, kg/sec
P_G	power transmitted to the gas, W

The power transmitted to the gas was the difference between the total net forward power (sum of the forward powers minus the sum of the reverse powers) and the coil power loss (I^2R). The coil power losses were determined separately by operating the engine with no plasma present. The coil power loss, as determined by the radio-frequency wattmeters, was approximately 11 percent higher than that calculated by the steady-state distilled-water temperature rise due to losses in uncooled portions of the electric circuit. Therefore, the coil power loss determined by the wattmeters was used in all the calculations.

An energy efficiency (or thermal efficiency) was computed from the measured cooling-water flow rate and temperature rise when the thrust drum was used as a calorimeter. The energy efficiency is given by

$$\eta_E = \frac{P_B}{P_G} \tag{2}$$

where P_B is the beam power determined calorimetrically.

The specific impulse I_{sp} was calculated from the measured thrust and propellant mass flow rate as

$$I_{sp} = \frac{T}{\dot{m}g} \tag{3}$$

Since thrust data and beam-power data could not be obtained simultaneously, some correlation was required to assign specific-impulse values to each beam-power data point. The correlation used in this report was obtained by plotting the power to the gas P_G as a function of the specific impulse for the thrust data, with the mass flow rate as a parameter. Specific-impulse values for the beam-power data could be estimated from these curves by knowing the power to the gas and the mass flow rate.

Effect of Engine Exhaust Pressure

Recent experimental results reported by Seikel (ref. 10) have indicated a significant dependence of thrustor performance on the ambient pressure at the thrustor exit. In an attempt to determine if the exit pressure affected the plasma engine performance, a short series of tests was conducted with the thrust target removed. Pressure reductions of the order of 30 percent were possible by this method. The pressure in the 6-inch tee with no thrust target was 6×10^{-4} torr at an argon flow rate of 1.06×10^{-6} kilogram per second. The power to the gas obtained in these tests was compared with the power obtained with the thrust target in place. At the same argon mass flow rates and coil currents, the measured power to the gas was approximately 15 percent lower when the thrust target was removed. No conclusion can be reached, however, regarding the effect of pressure on efficiency, since the relation between thrust and power into the gas is unknown for variable exhaust pressure.

RESULTS AND DISCUSSION

A brief summary of the data obtained during this investigation is given in table I. These data have met the requirement that the power transferred to the gas must be at least 20 percent of the total power (coil power plus power to the gas). This requirement

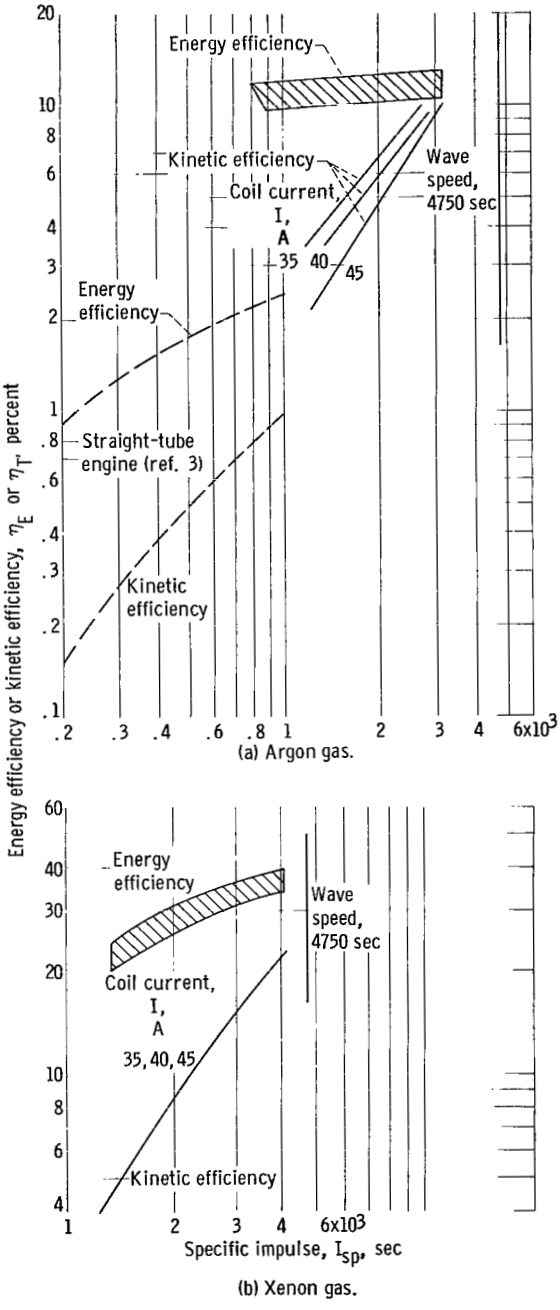

Figure 7. - Comparison of 4-coil engine performance.

was imposed to ensure that the maximum possible error in the computed value of the power to the gas was never more than 25 percent.

Effect of Flared-Tube Geometry

As previously mentioned, the first step taken to improve the performance of the traveling magnetic wave plasma engine was a redesign of the pyrex tube to reduce the heat losses near the exhaust. Figure 7(a) compares the kinetic and energy efficiencies for this engine with the results previously obtained with the straight-tube engine of reference 3. The maximum kinetic efficiency obtained with the straight-tube engine was 1 percent at a specific impulse of 1000 seconds. The redesign of the plasma engine increased both efficiency and specific impulse substantially. Maximum kinetic efficiency of 10 percent at a specific impulse of 3200 seconds was obtained. The energy efficiency improved from a value of 2.4 percent at 1000 seconds for the straight-tube engine to 12 percent at 3200 seconds. This improved engine performance is directly attributable to the use of the flared tube, which reduced the heat loss and made operation at higher specific impulse possible.

The kinetic efficiency exhibits a marked dependence on the coil current; however, no consistent trend was observable for the computed values of the energy efficiency, so these data are represented by the cross-hatched area of figure 7(a). The scatter in these data is due primarily to the difficulty of estimating the appropriate value of specific impulse to be assigned to each data point and the difficulty of setting an exact operating point corresponding

to a previously measured specific impulse. In no case did the measured values of the specific impulse exceed the value corrsesponding to the speed of the magnetic wave.

Effect of High-Molecular-Weight Propellant

The second technique used to reduce the heat losses was operation with a higher molecular weight propellant, thereby decreasing the diffusion rate of the plasma to the walls. Xenon gas with a molecular weight of 131.3 was chosen for the initial tests because of the ease of handling and metering and because xenon has the same chemical properties as argon (mol. wt., 39.9). Furthermore, the lower first ionization potential (12.1 V for Xe and 15.7 V for Ar) was expected to result in a greater initial degree of propellant ionization. The performance of the 4-coil engine using xenon as the propellant is shown in figure 7(b). The maximum kinetic efficiency has improved from a value of 10 percent with argon (fig. 7(a)) to a value of 22.5 percent with xenon at a specific impulse of 4200 seconds. Correspondingly, the energy efficiency has risen from 12 to 37 percent at a specific impulse of 4200 seconds. As expected, the heat losses to the pyrex tube walls were considerably reduced by operation with xenon gas. This can be readily illustrated by comparing the data for runs 23 and 51 shown in table I. At nearly identical operating conditions and power to gas, 843 watts were collected in the calorimeter when xenon was the propellant compared with 276 watts collected with argon gas. Consequently, more of the power input to the gas is retained in the exiting plasma stream when the higher molecular weight propellant, xenon gas, is used. Further indication of the lower heat loss with xenon was noted by the smaller temperature rise of the cooling-jacket water. The single kinetic-efficiency curve shown in figure 7(b) represents the best fit through the data obtained at 35, 40, and 45 amperes of coil current. No systematic dependency of kinetic efficiency on coil current was observable with xenon, as had been obtained with argon; however, the energy efficiency data are again shown as a band due to the scatter in the data.

A further advantage of operation with xenon gas over argon was that the use of the plasma source was not necessary even at the lowest power levels. The plasma discharge was at all times very stable, and the tuning and operation of the radio-frequency transmitters was greatly simplified.

Effect of Engine Length

The 10-coil traveling magnetic wave plasma engine was constructed to determine the effect of increased engine length on engine performance. Since the magnetic-field

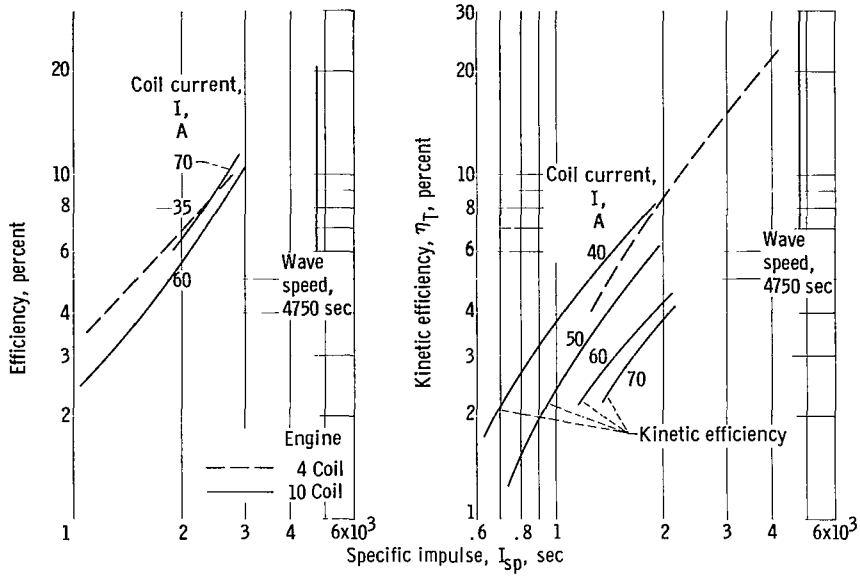

(a) Argon gas. (b) Xenon gas.

Figure 8. - Comparison of 4-coil and 10-coil engine performance.

coils had one-half the number of turns per coil that the 4-coil engine had, twice the coil current was required to maintain ampere-turns constant, and hence the axial magnetic field constant. The 10-coil engine had $2\frac{1}{2}$ magnetic-wave wavelengths available for plasma acceleration compared with the 1 wavelength for the 4-coil engine. Figure 8(a) compares the kinetic efficiency of the 10-coil engine with that obtained with the 4-coil engine at 35 amperes. Both engines used argon as the propellant. The 70-ampere curve appears to be an extension of the 35-ampere curve for the shorter engine. Engine performance is only slightly increased with the increased length. A maximum kinetic efficiency of approximately 11. 5 percent was obtained at a specific impulse of 2900 seconds.

Figure 8(b) compares the efficiency of the 10-coil engine with that of the 4-coil engine with xenon as the propellant. Under this condition, the performance of the 10-coil engine is reduced. The best performance obtainable at 70 amperes (equivalent to 35 A with the 4-coil engine) was a kinetic efficiency of 4. 1 percent at 2150 seconds impulse. A typical result with the 4-coil engine was 9. 5 percent at that specific impulse. A similar reduction in efficiency with increased engine length has been noted by Smotrich (ref. 4) with argon gas.

A possible reason for this reduced efficiency is that the plasma, once accelerated to near wave speed, is still within the engine and subsequently loses energy to the walls. Consequently, additional accelerator length beyond that required to achieve a plasma-beam specific impulse approaching that corresponding to the wave speed is detrimental. Further increases in accelerator length would result in reduced kinetic efficiency simply

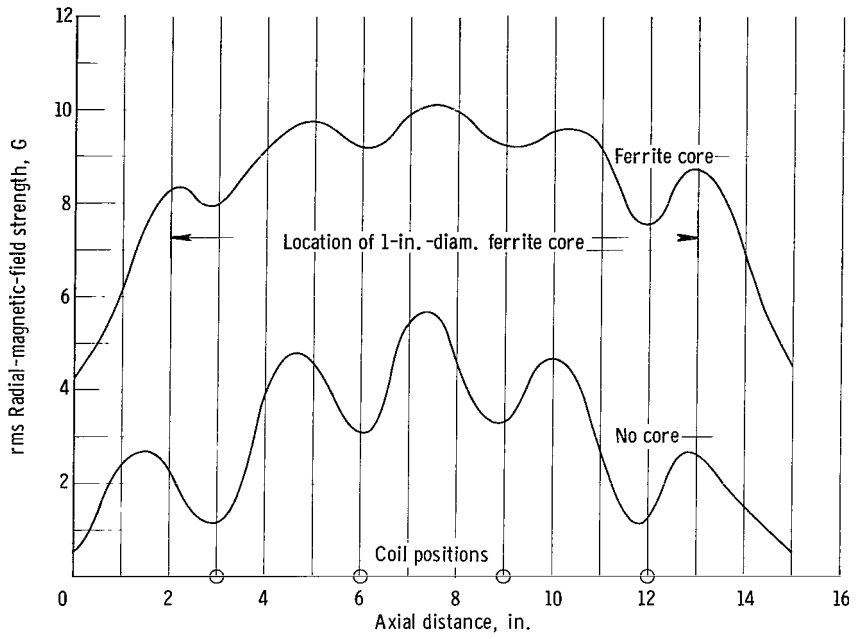

Figure 9. - Comparison of radial magnetic fields obtained with and without ferrite core at coil current of 30 amperes.

because no further increases in plasma velocity are possible while the energy losses to the walls increase.

These results suggest that, for any given propellant and wave speed, there is an optimum engine length that will maximize the engine efficiency and the plasma-beam specific impulse. Lengths shorter than the optimum value will produce low efficiency because the plasma is not accelerated to the maximum attainable velocity, while lengths longer than the optimum result in unnecessary wall losses. The two lengths investigated herein are not sufficient to estimate the optimum value for either of the propellants, although the fact that little change occurred in the argon indicates that the optimum length may be between the two investigated.

Effect of Ferrite Core

Radial component of magnetic wave. - The axial component of the magnetic flux density serves to induce an azimuthal current in the plasma. The interaction of this current with the radial component of the magnetic field produces the body force on the plasma that accelerates the plasma in the direction of the magnetic-wave motion. Thus, increased engine performance should result from increasing the strength of the radial component of the magnetic field. To accomplish this, a ferrite core was installed on the centerline of the 4-coil engine, and data were taken to determine the effectiveness of this core on engine performance. Figure 9 compares the rms values of the radial component of the magnetic field as measured with and without the ferrite core. The average

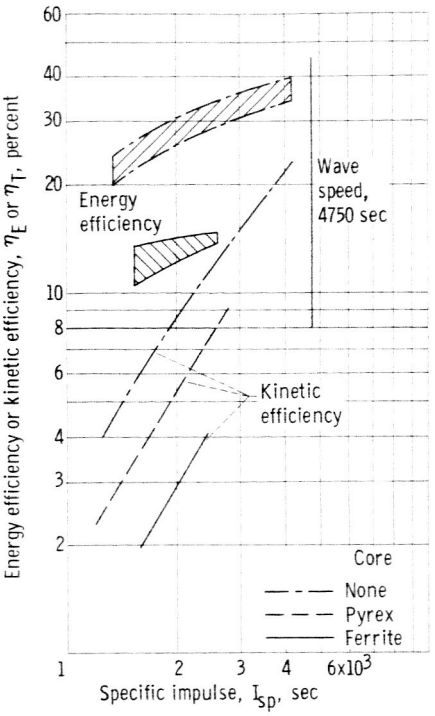

Figure 10. - Comparison of 4-coil engine performance with and without ferrite core with xenon gas. Coil current, 35 to 45 amperes.

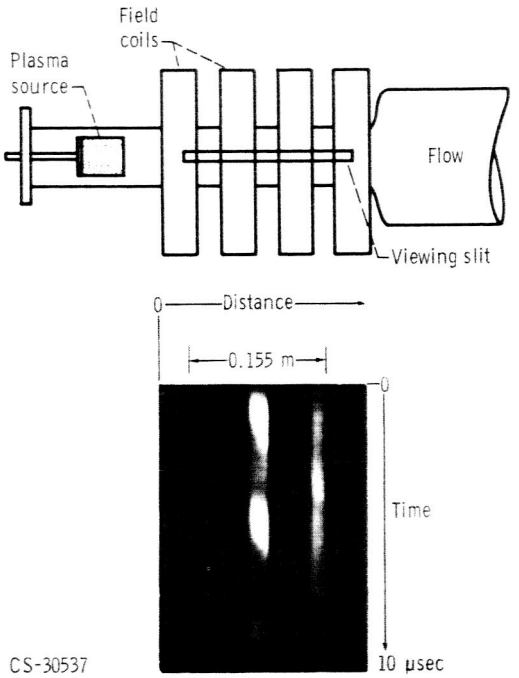

Figure 11. - Four-coil plasma engine showing location of viewing slit and typical streak photograph. Computed velocity, approximately 2.6×10^4 meters per second; wave speed, 3.75×10^4 meters per second.

intensity of the radial magnetic field is at least doubled by the presence of the ferrite core. The data for this figure were obtained by traversing a radial-magnetic-field pickup probe through the engine at a radius of 1/2 inch off the axis. For these measurements, the engine was operated at a constant magnetic-field coil current, and no plasma was present. The magnetic-flux-density profile obtained with the ferrite filled core is not only greater than the flux density obtained with an empty core, but also displays a flatter profile with distance through the engine. The smaller depression of the magnetic flux density at the coil positions is due to enhancement of the cross-coupling between the field coils through the ferrite core.

Engine performance. - Figure 10 compares the performance of the 4-coil engine with and without the ferrite core using xenon gas. Also shown is the kinetic efficiency obtained when the engine was tested with a pyrex-tube core. The curves shown in figure 10 were drawn as the best fit through the data taken over the indicated range of coil currents. As in figure 7, the energy-efficiency data are presented in a band due to data scatter and the difficulty of estimating the proper value of specific impulse for each data point. As can be seen, the performance has been considerably reduced by the addition of the pyrex core and is reduced even more by the ferrite core. The very low performance obtained with the ferrite core suggests that the enhanced radial component of the magnetic wave allowed greater diffusion of the plasma to the tube walls. This increased

loss apparently more than counterbalanced any gains due to improved interaction between the magnetic wave and the plasma. On the basis of these few tests, it seems doubtful that the use of a ferrite core will be beneficial.

The following table summarizes the best performance obtained with each of the reported engine configurations:

Engine configuration	Propellant	Maximum specific impulse, I_{sp}, sec	Maximum kinetic efficiency, η_T, percent	Maximum energy efficiency, η_E, percent
4-Coil (ref. 3)	Argon	1000	1.0	2.4
4-Coil (flared tube)	Argon	3200	10.0	12
	Xenon	4200	23.0	37
10-Coil (flared tube)	Argon	3000	[a]11.5	----
	Xenon	2150	[a]8.2	----
4-Coil				
(pyrex core)	Xenon	2700	8.6	----
(ferrite core)	Xenon	2450	4.1	14

[a]For these cases the maximum kinetic efficiency and specific impulse were not obtained at the same operating conditions.

Streak Photographs

Streak photography provided a qualitative comparison of the velocities obtained with the thrust target. These pictures were taken with a commercially available image-converter camera. The camera was used to take streak photographs both along the entire engine and in the region between the second and third coils. The 4-coil engine was altered for these tests so that the magnetic wave speed was 3.75×10^4 meters per second. Xenon gas was used as the propellant.

A drawing of the 4-coil plasma engine showing the location of the viewing slit is shown in figure 11 together with a streak photograph taken along the entire engine length. The engine was operated at a xenon mass flow rate of 1.87×10^{-6} kilogram per second and a coil current of 35 amperes. Over the exposure time period, 10 microseconds, three distinct, regularly spaced pulses of plasma can be seen traversing the engine. The regularity of the plasma pulses is expected, since one pulse should occur at each half-cycle of the magnetic wave (each 3.3 μsec when the frequency of the magnetic wave is 150 kc).

Figure 12(a) is a streak photograph taken between the second and third magnetic-field coils, showing one plasma pulse. The engine was operated at a xenon mass flow

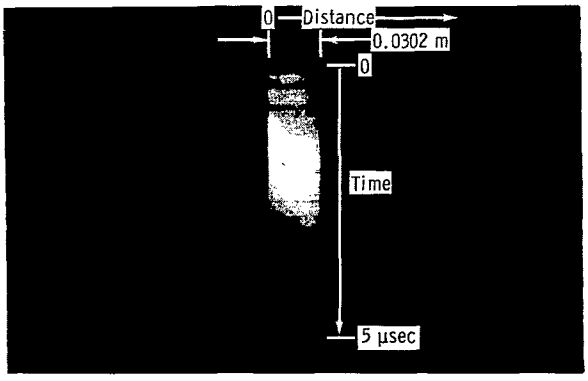

(a) Streak photograph. Current in second magnetic field coil, 25 rms amperes. Computed velocity, approximately 3×10^4 meters per second.

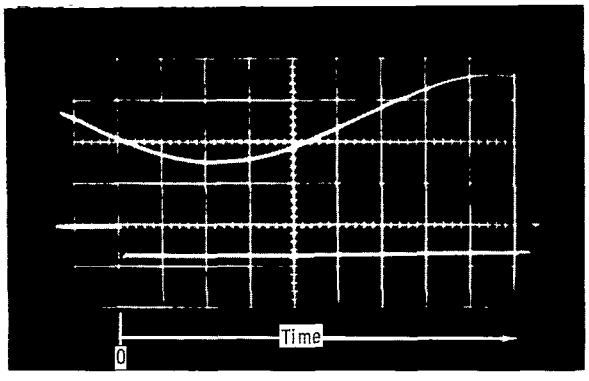

(b) Current trace. Camera shutter open.
Scale: 1 centimeter approximately equal to 0.5 microsecond.

Figure 12. - Streak photograph of engine using xenon gas. Camera view between second and third magnetic-field coils.

rate of 2.72×10^{-6} kilogram per second and a coil current of 30 amperes. Figure 12(b) is an oscillogcope trace showing the current in the second coil related to the time of the camera exposure in figure 12(a).

The lack of sharpness, the small size of the image, and the technical problems involved in enlargement made accurate determination of the plasma velocity difficult. The velocities given in figures 11 and 12 are computed from the best estimate of the streak slope. Approximately 30 streak photographs were taken and all yielded velocities between 65 and 90 percent of the magnetic speed. The definition of the streak photographs was not adequate to observe acceleration.

CONCLUDING REMARKS

The performance of the redesigned traveling magnetic wave plasma engine has been studied to determine the effect on the engine performance of flared-tube geometry, propellant molecular weight, engine length, and a ferrite core.

The flared-tube geometry removed the region of high heat loss to the tube walls with a resulting improvement in engine efficiency and specific impulse.

A high-molecular-weight propellant, such as xenon gas, gave increased kinetic efficiency over that obtained using argon gas for the 4-coil engine. From the data obtained it seems desirable to continue experimental testing with different molecular weight propellants and engine lengths in an attempt to increase the kinetic and energy efficiencies further.

There appears to be an optimum engine length that maximizes performance for any given propellant. For the two propellants tested, the one with higher molecular weight (xenon) produced the higher engine performance at the shorter engine length.

The use of a magnetic core material resulted in energy losses that greatly exceeded

any positive effect produced by improved interaction between the magnetic wave and the plasma.

Lewis Research Center,
National Aeronautics and Space Administration,
Cleveland, Ohio, December 9, 1964.

REFERENCES

1. Schaffer, Allan: Plasma Propulsion with a Pulsed Transmission Line. ARS Jour., vol. 31, no. 12, Dec. 1961, pp. 1718-1722.
2. Covert, Eugene E., and Haldeman, Charles W.: The Traveling-Wave Pump. ARS Jour., vol. 31, no. 9, Sept. 1961, pp. 1252-1260.
3. Jones, Robert E., and Palmer, Raymond W.: Traveling Wave Plasma Engine Program at NASA Lewis Research Center. Third Annual Conf. on Eng. Aspects of Magnetohydrodynamics, Univ. of Rochester, Mar. 28-29, 1962.
4. Smotrich, H., and Janes, G. Sargent: Experimental Studies of a Magnetohydrodynamic C. W. Traveling Wave Accelerator. Fourth Symposium on Eng. Aspects of Magnetohydrodynamics, Univ. of Calif., Apr. 1963.
5. Heflinger, Lee, and Schaffer, Allan: Magnetic Induction Plasma Engine. Rep. 1, (Clauser Tech. Corp.) General Tech. Corp., May 1962.
6. Heflinger, Lee, and Schaffer, Allan: Magnetic Induction Plasma Engine. Rep. 2, General Tech. Corp., May 31, 1963.
7. Keller, Thomas A.: NASA Electric Rocket Test Facilities. Trans. Seventh Nat. Symposium on Vacuum Tech., Am. Vacuum Soc., Inc., 1960, pp. 161-167.
8. Palmer, Raymond W., Jones, Robert E., and Seikel, George R.: Analytical Investigations of Coil-System Design Parameters for a Constant-Velocity Traveling Magnetic Wave Plasma Engine. NASA TN D-2278, 1964.
9. Domitz, Stanley: Experimental Evaluation of a Direct-Current Low-Pressure Plasma Source. NASA TN D-1659, 1963.
10. Seikel, George R., Bowditch, David N., and Domitz, Stanley: Application of Magnetic-Expansion Plasma Thrustors to Satellite Station Keeping an Attitude Control Missions. NASA TM X-52049, 1964.

TABLE I. - EXPERIMENTAL DATA

Run	Mass flow rate, $\dot{m}$, kg/sec	Coil current, I, A	Power to gas, P_G, W	Thrust, T, N	Beam power, P_B, W	Specific impulse, I_{sp}, sec	Kinetic efficiency, η_T, percent	Energy efficiency, η_E, percent
4-Coil four-phase engine; argon gas								
1	0.26×10^{-6}	35	1340	0.745×10^{-2}	---	2920	8.29	-----
2	.462	35	1760	1.255	---	2770	10.0	-----
3	↓	40	1980	1.255	---	2770	8.94	-----
4	↓	45	2270	1.215	---	2690	7.34	-----
5	↓	45	2475	1.46	---	3220	9.72	-----
6	.74	40	2210	1.175	---	1620	4.4	-----
7	↓	40	2540	1.42	---	1960	5.58	-----
8	↓	40	2390	1.09	---	1500	3.48	-----
9	↓	45	3050	1.215	---	1675	3.41	-----
10	↓	45	2790	1.52	---	2100	5.82	-----
11	1.10	35	3115	1.89	---	1750	5.35	-----
12	↓	35	2240	1.175	---	1180	3.43	-----
13	↓	40	3000	1.715	---	1590	4.65	-----
14	↓	45	4040	1.36	---	1240	2.14	-----
15	1.57	35	3465	2.38	---	1545	5.40	-----
16	1.57	40	4330	2.82	---	1830	6.06	-----
17	1.985	35	3750	2.52	---	1300	4.45	-----
18	.26	45	1680	----	162	2980	----	9.65
19	.462	35	1130	----	118	2650	----	10.45
20	.462	35	1080	----	111	2620	----	10.30
21	.462	40	1420	----	182	2700	----	12.80
22	.462	45	3030	----	336	2900	----	11.10
23	.462	45	2180	----	276	2800	----	12.65
24	.74	35	1810	----	193	960	----	10.65
25	.74	40	3470	----	391	2850	----	11.25
26	.74	45	3630	----	408	3150	----	11.25
27	1.10	35	3180	----	462	1850	----	14.50
28	1.10	40	3470	----	326	2150	----	9.40
29	1.10	45	4050	----	482	2820	----	11.90
30	1.48	35	2630	----	262	1140	----	9.95
31	1.48	40	3260	----	409	1420	----	12.55
32	1.985	35	2880	----	327	850	----	11.35

TABLE I. - Continued. EXPERIMENTAL DATA

Run	Mass flow rate, $\dot{m}$, kg/sec	Coil current, I, A	Power to gas, P_G, W	Thrust, T, N	Beam power, P_B, W	Specific impulse, I_{sp}, sec	Kinetic efficiency, η_T, percent	Energy efficiency, η_E, percent
4-Coil four-phase engine; xenon gas								
33	0.21×10^{-6}	35	1078	0.785×10^{-2}	---	3810	13.6	----
34	.21	40	880	.856	---	4170	19.9	----
35	.21	45	1310	.906	---	4410	15.0	----
36	.425	35	1095	1.35	---	3240	19.6	----
37	.425	40	1125	1.52	---	3650	24.2	----
38	.425	45	1560	1.57	---	3770	18.7	----
39	.61	35	1410	1.42	---	2380	11.8	----
40	.61	40	2100	1.47	---	2460	8.5	----
41	.61	45	2120	1.57	---	2625	9.2	----
42	.815	35	1545	1.52	---	1900	9.2	----
43	.815	40	2155	1.62	---	2025	7.5	----
44	.815	45	1875	1.57	---	1965	8.1	----
45	1.715	35	3450	2.20	---	1310	4.12	----
46	1.715	40	3480	2.33	---	1385	4.55	----
47	1.715	45	3685	2.60	---	1545	5.35	----
48	2.64	35	4990	3.53	---	1365	4.70	----
49	.425	35	1645	----	556	3880	----	33.6
50	.425	40	2040	----	730	4000	----	35.8
51	.425	45	2260	----	843	4100	----	37.3
52	.61	35	2285	----	665	2650	----	29.1
53	.61	40	2610	----	776	2710	----	29.7
54	.61	45	2690	----	909	2740	----	33.8
55	.815	35	2555	----	722	2120	----	28.2
56	.815	40	2610	----	866	2150	----	33.2
57	.815	45	3330	----	953	2850	----	28.6
58	1.715	35	3835	----	855	1400	----	22.6
59	1.715	40	4370	----	990	1470	----	25.0
60	1.715	45	4640	----	1160	1500	----	25.0

TABLE I. - Continued. EXPERIMENTAL DATA

Run	Mass flow rate, $\dot{m}$, kg/sec	Coil current, I, A	Power to gas, P_G, W	Thrust T, N	Beam power, P_B, W	Specific impulse, I_{sp}, sec	Kinetic efficiency, η_T, percent	Energy efficiency, η_E, percent
10-Coil four-phase engine; argon gas								
61	0.30×10^{-6}	60	1340	0.882×10^{-2}	---	3000	9.70	----
62	.40	60	1690	1.167	---	2980	10.10	----
63	.50	60	1900	1.225	---	2500	7.90	----
64	.60	60	1840	1.334	---	2230	8.05	----
65	.60	70	2080	1.656	---	2820	11.15	----
66	.70	60	2460	1.46	---	2130	6.19	----
67	.70	70	2260	1.618	---	2360	8.28	----
68	1.00	60	2820	1.588	---	1610	4.47	----
69	1.00	70	3210	2.110	---	2125	6.93	----
70	1.30	60	3180	1.82	---	1430	4.13	----
71	1.30	70	3780	2.47	---	1940	6.49	----
72	1.60	60	3740	1.755	---	1120	2.58	----
73	2.00	60	4410	2.080	---	1060	2.45	----
10-Coil four-phase engine; xenon gas								
74	0.40×10^{-6}	40	820	0.726×10^{-2}	---	1850	8.00	----
75	.40	50	1280	.726	---	1850	5.15	----
76	.40	60	1900	.824	---	2100	4.50	----
77	.516	40	1030	.873	---	1725	7.15	----
78	.516	50	1450	.931	---	1840	5.77	----
79	.516	60	2790	1.050	---	2070	3.82	----
80	.516	70	2830	1.080	---	2130	4.14	----
81	.60	40	1050	.774	---	1315	4.75	----
82	.60	50	1270	.843	---	1435	4.65	----
83	.60	60	1710	.902	---	1530	3.95	----
84	.60	70	2525	.804	---	1365	2.22	----
85	1.00	40	1630	1.08	---	1100	3.60	----
86	1.00	50	2010	1.315	---	1340	4.25	----
87	1.00	60	3830	1.480	---	1510	2.85	----
88	1.40	40	1640	1.185	---	865	3.05	----
89	1.40	50	2920	1.470	---	1070	2.65	----
90	1.40	60	3940	1.685	---	1230	2.57	----
91	2.00	40	2360	1.295	---	660	1.75	----
92	2.00	50	3520	1.685	---	860	2.00	----
93	2.00	60	4720	2.160	---	1100	2.47	----
94	2.40	40	2370	1.460	---	620	1.87	----
95	2.40	50	5250	1.862	---	790	1.37	----

TABLE I. - Concluded. EXPERIMENTAL DATA

Run	Mass flow rate, $\dot{m}$, kg/sec	Coil current, I, A	Power to gas, P_G, W	Thrust, T, N	Beam power, P_B, W	Specific impulse, I_{sp}, sec	Kinetic efficiency, η_T, percent	Energy efficiency, η_E, percent
4-Coil four-phase engine; xenon gas; pyrex core								
96	0.425×10^{-6}	45	1740	1.13×10^{-2}	---	2700	8.7	----
97	.610	45	2010	1.22	---	2050	6.1	----
98	.815	45	2960	1.48	---	1860	4.5	----
99	1.715	40	5050	2.01	---	1195	2.3	----
4-Coil four-phase engine; xenon gas; ferrite core								
100	0.425×10^{-6}	35	3100	0.785×10^{-2}	---	1880	2.34	----
101	.425	40	2900	.905	---	2180	3.3	----
102	.425	45	2900	1.00	---	2420	4.1	----
103	.61	35	3680	1.03	---	1720	2.4	----
104	.61	40	3810	1.03	---	1720	2.3	----
105	.61	45	4120	1.055	---	1760	2.2	----
106	.815	35	5040	1.275	---	1600	1.98	----
107	.815	40	5450	1.37	---	1720	2.20	----
108	.815	45	5500	1.37	---	1720	2.18	----
109	.425	35	3240	-----	431	1920	----	13.3
110	.425	40	3650	-----	486	2280	----	13.3
111	.425	45	3760	-----	525	2560	----	14.0
112	.61	35	4540	-----	525	1720	----	11.6
113	.61	40	4530	-----	591	1740	----	13.0
114	.61	45	4620	-----	635	1765	----	13.7
115	.815	35	5530	-----	623	1610	----	11.3
116	.815	40	5080	-----	668	1670	----	13.1
117	.815	45	5020	-----	754	1750	----	15.0

2/22/85

"The aeronautical and space activities of the United States shall be conducted so as to contribute . . . to the expansion of human knowledge of phenomena in the atmosphere and space. The Administration shall provide for the widest practicable and appropriate dissemination of information concerning its activities and the results thereof."

—NATIONAL AERONAUTICS AND SPACE ACT OF 1958

NASA SCIENTIFIC AND TECHNICAL PUBLICATIONS

TECHNICAL REPORTS: Scientific and technical information considered important, complete, and a lasting contribution to existing knowledge.

TECHNICAL NOTES: Information less broad in scope but nevertheless of importance as a contribution to existing knowledge.

TECHNICAL MEMORANDUMS: Information receiving limited distribution because of preliminary data, security classification, or other reasons.

CONTRACTOR REPORTS: Technical information generated in connection with a NASA contract or grant and released under NASA auspices.

TECHNICAL TRANSLATIONS: Information published in a foreign language considered to merit NASA distribution in English.

TECHNICAL REPRINTS: Information derived from NASA activities and initially published in the form of journal articles.

SPECIAL PUBLICATIONS: Information derived from or of value to NASA activities but not necessarily reporting the results of individual NASA-programmed scientific efforts. Publications include conference proceedings, monographs, data compilations, handbooks, sourcebooks, and special bibliographies.

Details on the availability of these publications may be obtained from:

SCIENTIFIC AND TECHNICAL INFORMATION DIVISION

NATIONAL AERONAUTICS AND SPACE ADMINISTRATION

Washington, D.C. 20546